Title: Boosting oxygen and peroxide reduction reactions on PdCu Intermetallic Cube

Authors: Qingfeng Zhang; Fan Li; Lina Lin; Jiaheng Peng; Wencong Zhang; Wenlong Chen; Qian Xiang; Fenglei Shi; Wen Shang; Peng Tao; Chengyi Song; Rong Huang; Hong Zhu; Tao Deng; Jianbo Wu

To be cited as: ChemElectroChem 10.1002/celc.202000381

Link to VoR: https://doi.org/10.1002/celc.202000381

Boosting oxygen and peroxide reduction reactions on PdCu Intermetallic Cube

Qingfeng Zhang[a], Fan Li[a], Lina Lin[b], Jiaheng Peng[a], Wencong Zhang[a], Wenlong Chen[a], Qian Xiang[a], Fenglei Shi[a], Wen Shang[a], Peng Tao[a], Chengyi Song[a], Rong Huang*[b], Hong Zhu[a,c,d], Tao Deng[a,d,e], Jianbo Wu*[a,d,e]

[a] Q.Zhang, F.Li, J.Peng, W.Zhang, Dr.W.Chen, Q.Xiang, F.Shi, Prof.W.Shang, Prof.P.Tao, Prof.C.Song, Prof.H.Zhu, Prof.T.Deng, Prof.J.Wu
State Key Laboratory of Metal Matrix Composites
School of Materials Science and Engineering
Shanghai Jiao Tong University
800 Dongchuan Rd, Shanghai, 200240 (China)
E-mail: jianbowu@sjtu.edu.cn

[b] L.Lin, Prof.R.Hong
Key Laboratory of Polar Materials and Devices (MOE) and Department of Electronics
East China Normal University
Shanghai 200062 (China)
E-mail: rhuang@ee.ecnu.edu.cn

[c] Prof.H.Zhu
University of Michigan – Shanghai Jiao Tong University Joint Institute
Shanghai Jiao Tong University
800 Dongchuan Road, Shanghai, 200240 (China)

[d] Prof.H.Zhu, Prof.T.Deng, Prof.J.Wu
Materials Genome Initiative Center
Shanghai Jiao Tong University
800 Dongchuan Road, Shanghai 200240 (China)

[e] Prof.T.Deng, Prof.J.Wu
Center of Hydrogen Science
Shanghai Jiao Tong University
800 Dongchuan Road, Shanghai 200240 (China)

Supporting information for this article is given via a link at the end of the document.((Please delete this text if not appropriate))

Abstract: The palladium-based nano-catalysts have the tendency to replace the platinum-based catalysts for fuel-cell reaction in alkaline electrolytes, especially PdCu intermetallic nanoparticles with high electrochemical activity and stability. However, unlike the synthetic method of nanoparticles, the shape effect in the performance was relatively less studied. Here, we demonstrate that the facet dependence of PdCu intermetallics on oxygen reduction reaction (ORR) and peroxides reduction and reveal the {100} dominant PdCu cube had much higher ORR mass activity and specific activity than spheres at 0.9V vs. RHE, which is 4 and 5 times of commercial Pd/C and Pt/C catalysts, and shows only a 31.7% decay after 30000 cycles stability test. Moreoer, cubic PdCu nanoparticles show higher peroxide electroreduction activity than Pd cubes and PdCu spheres. The density functional theory (DFT) reveals that the huge difference originates from the reduction of oxygen absorption energy and energy barrier of peroxide decomposition on order {100} PtCu surface. Given the relation between shape and electrochemical performance, this study can benefit the further research on electro-catalytic improvement of catalysts in alkaline environment.

Introduction

The platinum-based catalysts are highly pivotal for the electrochemical reactions[1], especially for the sluggish oxygen reduction reaction in proton exchange membrane fuel cell (PEMFC)[2],[3]. As the honeypot for the fuel-cell catalysts, many researches focused on the boosts of the activity[4],[5] and durability[6],[7] of these catalysts by morphology[8],[9],[10] and composition engineering. However, the scarce world reserves, high cost and poor long-term duration restrict their wide applications[11]. Besides, the major problem with platinum-group metals is the low activity in alkaline environment because of the difficulty in achieving the optimized oxygen binding strength on these catalysts in the presence of hydroxide[12]. Among the other noble metal catalysts, Pd and Pd-based alloys can become the promising electrocatalysts in alkaline environment[13],[14],[15]. The other oxygen relevant electrochemical reaction, hydrogen peroxide electroreduction, can also be powered by Pd-based catalysts[16]. The hydrogen peroxide plays an important role in the living cells and its concentration at the normal level can maintain the health of the living body[17]. In the previous study, Pt and Pt-based nanocomposites were wildly used for catalysts[18]. To reduce its cost, Pd-based nanocatalysts were investigated and showed impressive performance, such as PdPt[19], PtPd-Fe_3O_4[20], Pd-Au[16]. In order to reduce the cost, the cheaper nanocatalysts, PdCu, may show its potential in this reaction.

The catalytic activity of noble metals can be improved through alloying by achieving the optimized oxygen binding strength. In recent years, many Pd-based catalysts have been reported with the catalytic performance comparable to or even superior to that of the commercial Pt/C, such PdNi[21], PdCo[22], PdFe[23],[24], PdW[25], and PdCu[26]. Among these bimetallic nanocatalysts, PdCu alloy received much attention for its high electrochemical activity and low cost[27],[28]. Many efforts have been focused on the control on the size, composition, shape and core-shell structure to boost its ORR activity[29],[30],[31],[32]. However, previous studies mainly focused on its A1 phase with disordered structure. Such random alloy suffers from poorer stability compared with Pt-based nanocrystals in corrosive environment. Different with the conventional disordered structure,the ordered structure with fixed atom positions and site occupancies shows great stability due to the formation of uniform heteroatomic bonding[33],[34].

Inspired by this, the ordered B2 phase of PdCu with intermetallic structure was engineered to achieve this prospect by the seed-mediated co-reduction route[35], high temperature annealing[36],[37] or one-step liquid reduction method[38],[39]. Very few works could synthesize the faceted PdCu intermetallics regarding both durability and activity. Recently, Sara E. Skrabalak et al. have reported the enhanced activity and stability for oxygen reduction reaction of PdCu intermetallic cube compared with the random alloy[35],[40]. Nevertheless, few studies have reported the comparison of PdCu ordered alloys with different shapes in electrochemical performance and explained the origin of the enhancement of the oriented ordering on performance.

In this work, we successfully synthesized two shapes of PdCu intermetallics, cubes and sphere, by slightly modifying the reported method[41] and investigated the effect of faceted and ordering on their electrochemical properties in both ORR and hydrogen peroxide reduction reaction. The PdCu cube/C shows the large improvement in both ORR and peroxide reduction. The PdCu cube shows up to 5 times improvement in mass activity towards ORR while the PdCu sphere just shows almost same activity compared with the commercial Pt/C catalysts. For H_2O_2 reduction, the PdCu cube shows the enhancement of up to 8.4 times for mass activity compared with the PdCu sphere. The DFT calculation reveals that huge difference originates from the reduction of oxygen absorption energy and energy barrier of peroxide decomposition on order {100} PtCu surface.

Results and Discussion

Nanoparticles synthesis and structural characterization

Two catalysts for comparison were prepared by the same capping reagent (TPP) with different amounts. The size and Pd-to-Cu ratio of two particles remained nearly constant in order to compare shape-induced difference (Figure.1 and Table S1).

Figure.1a and Figure.1b show the monodisperse PdCu intermetallic nanocubes and nanospheres with average size of 11.57nm and 10.58nm, respectively. To further prove the intermetallic phase, HAADF-STEM, HRTEM and XRD were utilized to confirm the ordered PdCu structure. The atomic spacing of 0.297nm and 0.210nm in the STEM image of a single PdCu nanocube (inset in Figure.1a) and HR-TEM image of a single nanosphere (inset in Figure.1b) are correspond to the (100) and (110) plane of PdCu B2 phase[42], respectively, which

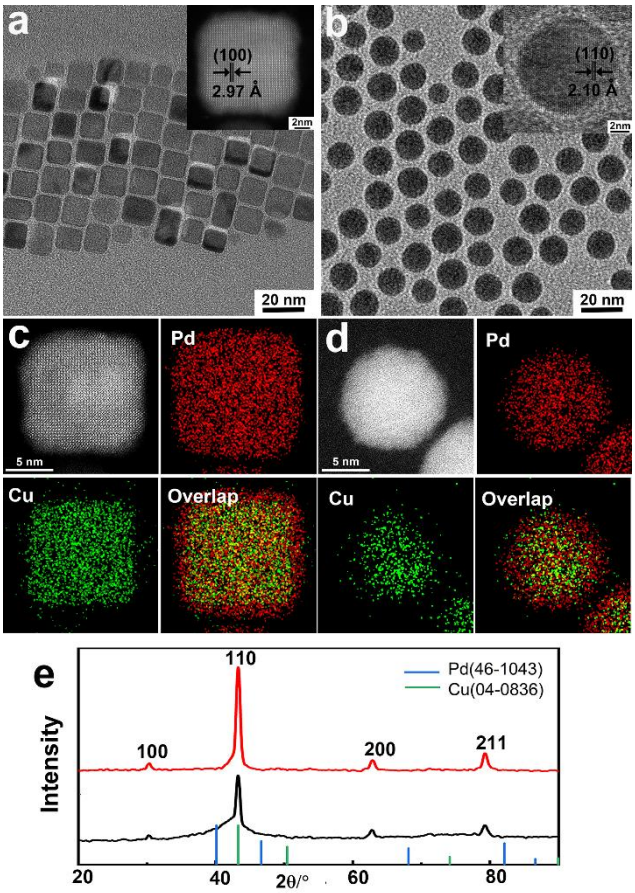

is consistent with the (100) and (110) spacings from XRD pattern (Figure.1e).

From the EDS mapping (Figure.1c and Figure.1d), the Pd and Cu elements distribute uniformly, which confirms the formation of PdCu alloy. The cubic and spherical PdCu nanocrystals were evaluated by ICP, indicating that Pd and Cu were almost identical in content (Tabel.S1), which is consistent with the elemental ratio of PdCu B2 ordered phase.

The temperature played a significant part in the synthesis of cubic PdCu nanoparticles. The monodispersed PdCu nanocubes could be obtained at 170°C.When heated to 180 and 200°C, some of cubes would turn into spheres due to the weak control of capping agent on the diffusion of Pd and Cu atoms at higher temperature (Figure.S1a and Figure.S1b). Thus, the final product was composed of all of spheres with size of 18nm when temperature reached 220°C, indicating capping reagent lost its shape-controlled ability completely because of the rapid diffusion rate (Figure.S1c).

Figure.1 Characterization of morphology and composition of PdCu nanoparticles. TEM images of (a) cubes (b) spheres. Atomic-resolution HAADF-STEM images of PdCu cubes and HR-TEM image of PdCu spheres are inserted in (a) and (b), respectively. EDS mappings of (c) cubes and (d) spheres. (e) XRD patterns of PdCu cubes and spheres.

Electrochemical Evaluation

To investigate the differences in electrochemical performance of these two PdCu nano-catalysts, the ORR and hydrogen peroxide reduction reaction were both tested.

Around 10nm Pd cubes prepared by reported method[43] (Figure.S2), the commercial Pt/C and Pd/C were used for comparative study. The CV tests were taken to activate the catalysts surface before the electrochemical measurement (Figure.S3). The electrochemical active surface areas (ECSA) of Pd-based catalysts were calculated by CO stripping method[44],[45], except the commercial Pt/C, that of which was determined by integrating hydrogen absorption–desorption region in the cyclic voltammetry (CV) curves (Figure.S3-S9). The PdCu cubes and spheres exhibit the ECSA of 59.4 m^2/g_{Pd} and 39.4 m^2/g_{Pd}, which are comparable to that of the commercial Pt/C (63.2 m^2/g_{Pt}).

ORR measurements were carried out by rotating disk electrodes (RDE) in the 0.1M O_2-saturated KOH solution. The LSV curves are shown in Figure.2a. The PdCu B2 cube/C shows slightly higher onset (0.941eV) and half-wave potential (0.896 eV) than Pd cube/C, much higher than PdCu sphere/C, commercial Pt/C and Pd/C catalysts. Figure.2b compares the specific and mass activities of all the nanocatalysts at 0.9V (vs.RHE). The specific activity was 0.42mA cm^{-2}_{Pd} for PdCu cube/C, which is slightly higher than that of Pd cubes (0.41 mA cm^{-2}_{Pd}), 3, 4, and 5 times as high as that of PdCu sphere/C (0.14 mA cm^{-2}_{Pd}), Pd/C (0.12 mA cm^{-2}_{Pd}), and Pt/C (0.08 mA cm^{-2}_{Pt}), respectively. The mass activity of PdCu cube/C reaches 0.25A mg^{-1}_{Pd}, which is about 28% higher than that of Pd cube/C (0.18A mg^{-1}_{Pd}), 5, 4, and 5 times higher than that of PdCu sphere/C (0.54A mg^{-1}_{Pd}), Pd/C (0.61A mg^{-1}_{Pd}) and Pt/C (0.56A mg^{-1}_{Pt}). The PdCu cube/C performs better than Pd cube/C due to the alloying Cu and contributing to the decrease of oxygen adsorption[46]. The superior performance of PdCu cube/C than sphere might be ascribed to its advanced PdCu ordered atomic arrangement on PdCu {100}.

The stability of all the catalysts were measured by accelerated durability test (ADT) in Ar-purged 0.1M KOH (Figure 2c-2d and Figure S10). The negative shifts of both the half-wave and the onset potential can be observed in Figure.2c due to the aggregation and etching of particles and change of shapes after 30000 cycles[47]. Figure.2d shows that the mass activity of PdCu cube/C decreases to 0.17A mg^{-1}_{Pd} with a loss of 31.7%, but still higher than that of Pd cube/C (0.10A mg^{-1}_{Pd}, 44.6% loss) and PdCu sphere/C (0.03A mg^{-1}_{Pd}, 41.3% loss). The commercial Pt/C only remains 38.6% of its initial mass activity, indicating the ordering atomic arrangement of PdCu nanoparticles could prevent the Cu leaching, and therefore enhance durability[40]. The low-indexed PdCu {100} shows less the surface defects than that on the higher indexed surface of sphere, which leads to the supreme durability over PdCu sphere. It is quite interesting that the PdCu intermetallic cube shows better stability even than Pd cube. From the EDS mapping image (Figure.1c), there is the ultrathin Pd skin on the PdCu cube, making the cube like the core-shell structure. The Pd out layer is under the tensile strain induced from the different interplanar crystal spacing between PdCu and Pd[48],[49]. The Pd atomic layers near surface can get closer to each other when stretched, making the surface of this stucture more dense than that of pure Pd cube. Thus, this tensile strain may enhance the PdCu cubes durability (Figure.S11). Although Pd/C only losts 36.3% of initial mass activity, its striking negative shift to half-wave potential and extremely low limited current hinder its application (Figure.S10). Thus, the ADT results indicate the PdCu cube/C has the best stability in alkaline environment among the tested samples.

The advantage of PdCu cube/C in H_2O_2 reduction reaction, was conducted in Ar-saturated 0.1M phosphate buffered saline (PBS). Figure.3a shows the CV curves of PdCu cube/C, PdCu sphere/C and Pd cube/C with and without H_2O_2. The obvious enhanced reduction peak can be observed after addition of H_2O_2, confirming the current is generated by catalytic reduction of H_2O_2[20]. The reduction peak currents of catalysts were normalized on loading noble metal to compare their mass activity (Figure.3b). The mass activity of PdCu cube/C was 0.042 mA/g, which is 1.6 times than that of Pd cube/C (0.026 mA/g) and 8.4 times than that of PdCu sphere/C (0.005 mA/g). Compared with the Pd cube, the enhanced performance of the PdCu may result from the synergistic effect[18]. The presence of

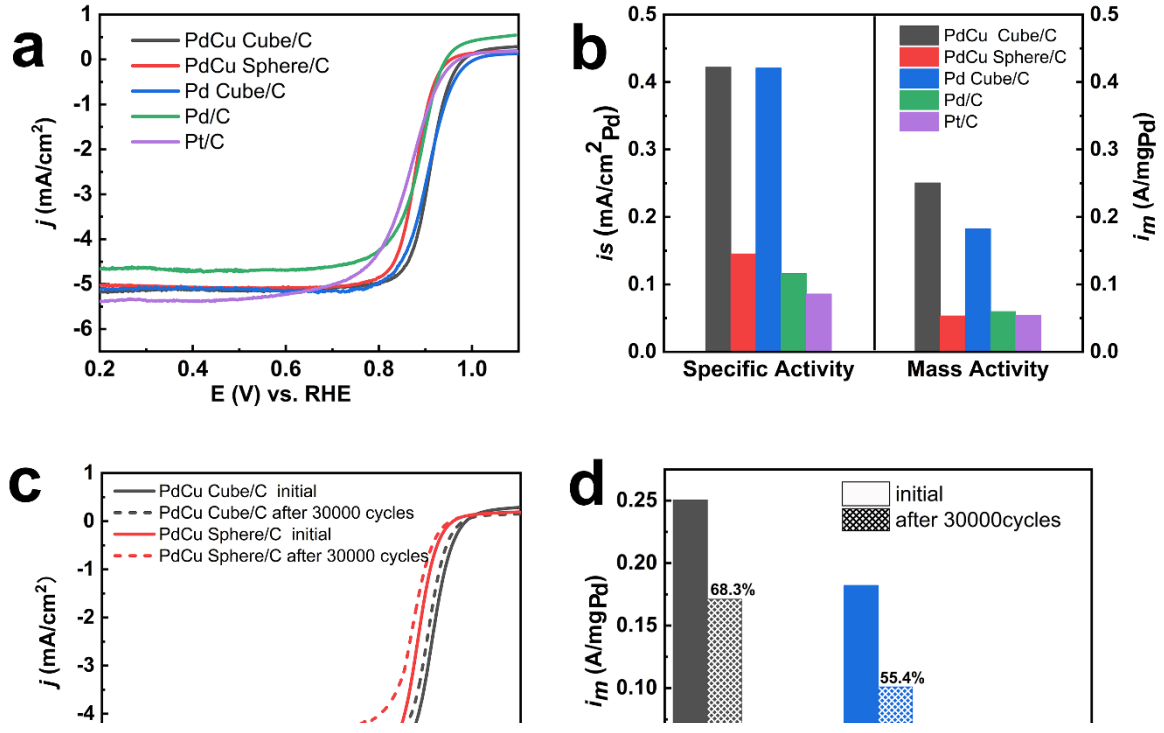

Figure.2 Electro catalytic performance of PdCu cubes, spheres, Pd cubes, commercial Pd/C and Pt/C. (a, b) ORR polarization curves (a) and comparison of the mass and specific activities (b) of the stated catalysts in 0.1 M KOH at 0.9 V versus RHE. (c, d) ORR polarization curves (a) and the mass activity change (d) of stated catalyst before and after 30000 cycles.

Cu could increase the adsorption sites for –OH species because it can reduce the strength of Pt–OH formation. The reduction peak current augments when increasing the amount of H_2O_2, further confirming the catalytic ability (Figure.3c). The liner relationship can be obtained according to CV curves when the concentration of H_2O_2 increases from 5 to 25 mM, which suggests its potential as hydrogen peroxide sensor[50]. Meanwhile, the cathodic peak currents increase when the sweep rate increases (Figure.3d). The liner relationship as the inserted image shows suggests that the H_2O_2 reduction is the typical diffusion-controlled process[51].

Based on the previous research[52], the oxygen in the oxygen reduction reaction is reduced either directly to the water (four electrons reaction) or to peroxide (two electrons reaction). The latter is preferred on the Pd and Pd-based alloys according to recent studies[53].

As discussed in the studies[15], the coverage of the hydroxyl species (OHad) shrinks the activate site for absorption of oxygen. The superior activity of PdCu cubes can be attributed to low coverage of the OH_{ad} [1]. The process of adsorption and desorption of oxygen or hydroxyl was found to be the determining step of the ORR[54]. Generally, the oxygen absorption energy can be used to evaluate the ORR activity. To further uncover the mechanism, density functional theory (DFT) was used for calculating the oxygen absorption energy (E_o) that was wildly used for measuring the ORR activity (see the details in Supporting information). The PdCu (100) and (110) slabs were built to represent the cubic and spherical PdCu model on the base of the corresponding HAADF-STEM and HRTEM images (Figure.S12)[55].

We compared the oxygen absorption energy between the cubic and spherical PdCu particles (Figure.4a and 4b). The E_o of the PdCu cube is -1.082eV, which is smaller than that of the sphere (-1.182eV), suggesting that PdCu cubes show higher ORR activity according to the volcano plot in the previous study[54].

For peroxide reduction reaction, according to the literature[56], the rate-determining step is as follows (Equation (1)),

$$H_2O_2{}^* + e^- = OH^- + OH^* \quad (1)$$

Similarly, PdCu (100) and (110) slabs were utilized to calculate the energy barrier of the rate-determining step of PdCu cubes and spheres, respectively (Figure.4c and 4d). The PdCu cubes are thermodynamically favorable for peroxide reduction reaction while spheres catalyze this reaction with the energy barrier. This calculation suggests that the cubes had better activity in peroxide reduction reaction. Thus, corresponding to the

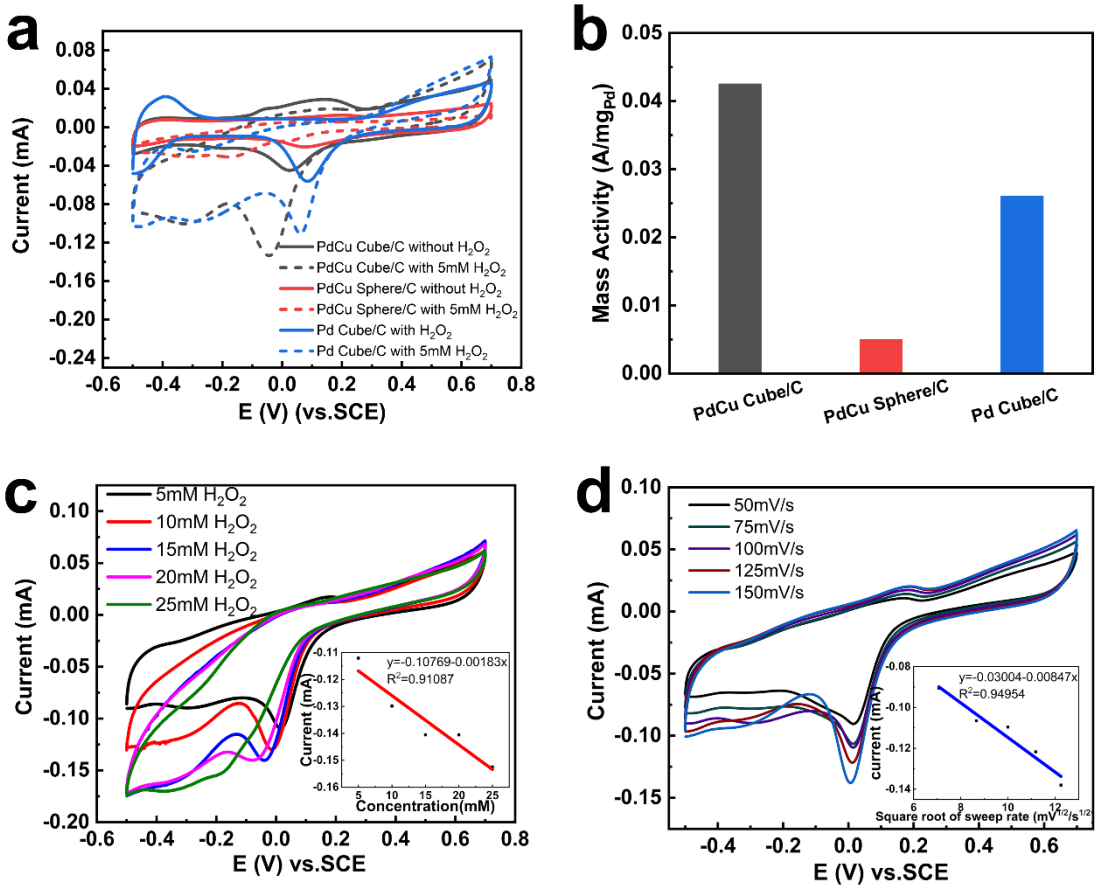

Figure.3 H_2O_2 reduction performance of PdCu cubes, spheres, Pd cubes. CV curves (a) and comparison of the mass activities (b) of the catalysts in 0.1M PBS solution. (c)CV curves of PdCu cubes in 0.1M PBS with different H_2O_2 concentration (sweep rate is 100mV/s), the inset shows the corresponding liner relationship. (d) CV curves of PdCu cubes in 0.1M PBS with 0.5mM H_2O_2 concentration at different sweep rates, the inset shows the corresponding liner relationship.

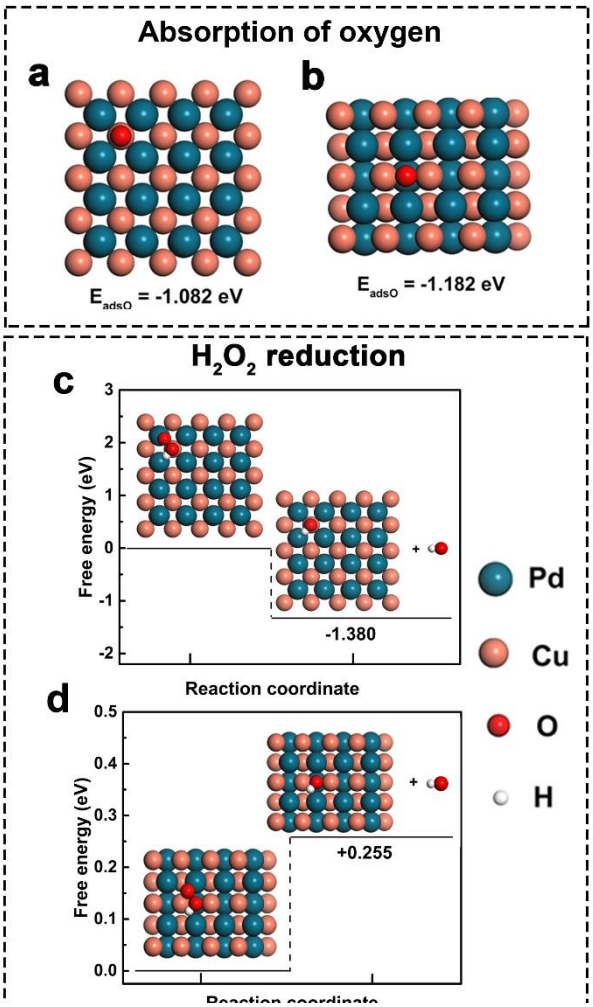

Figure.4 DFT models and results of ORR and H2O2 reduction (a) Stable adsorption site of the ORR determining intermediates, O, for PdCu (100) surface slab and the matched binding energy. (b) Stable adsorption site of the ORR determining intermediates, O, for PdCu (110) surface slab and the matched binding energy. (c) The energy barrier of peroxide reduction reaction's rate-determining step and the stable adsorption conFigureuration of H_2O_2, left HO on the surface of PdCu (100) slab.(d) The energy barrier of peroxide reduction reaction's rate-determining step and the stable adsorption conFigureuration of H_2O_2, left HO on the surface of PdCu (110) slab.

experimental results, our calculation results confirm the shape-induced influence on the electrochemical performance of PdCu particles.
Main Text Paragraph.

Conclusion

We have demonstrated the facet dependence of PdCu intermetallics on ORR and hydrogen peroxides reduction and revealed the {100} dominant PdCu cube shows superior performance than spheres in both ORR and H_2O_2 reduction reaction. Owing to their intermetallic phases, the PdCu cubes exhibit 5 times improved activity of and stability with only 31.7% loss after 30000 cycles in ORR and 8.4 times enhancements in H_2O_2 reduction compared to PdCu sphere. DFT calculation has uncovered that the dominant {100} crystal faces in cubes had more appropriate oxygen adsorption and more thermodynamically favorable for peroxide reduction than that of spheres. Therefore, our demonstration of the Pd based intermetallics reveal the extended application of Pd based catalysts in the improvement of electro-catalytic performance.

Experimental Section

Materials

Oleylamine(80-90%,OLA),Sodiumtetrachloropalladate(II) (Na_2PdCl_4,99.99%), Triphenylphosphine (TPP, ＞ 99.0%,GC) were purchased form Aladdin Industrial Inc.Copric chloride dehydrate ($CuCl_2{\cdot}2H_2O$, 99.99%) was purchased form Macklin Industrial Inc. Bis(acetylacetonato)palladium(II) ($Pd(acac)_2$) was purchased form Chengdu Boon Stream Chemical Industry Co. Ltd. Toluene(AR) and potassium bromide (KBr, AR) were purchased from Sinopharm group chemical reagent co. LTD.N-butylamine (＞90%) was obtained from TCI reagent company. 5wt.% Nafion solution, Perchloric acid ($HClO_4$,99.999%), Ascorbic acid (AA), poly(vinylpyrrolidone) (PVP, Mw≈55,000) were purchased from Aldrich. 10% Pd/C and 20% Pt/C were obtained form Alfa Aesar. High pure argon (Ar, 99.999%) was obtained from Shanghai Weichuang Standard Gas Company. Vulcan XC-72R carbon was obtained from Cabot Company. All chemicals were used without any further purification.

Synthesis of the PdCu intermetallic nanoparticles

For the synthesis of the cubic PdCu nanoparticles, a modified literature procedure was used. Typically, 0.1 mmol of $Pd(acac)_2$, 0.4 mmol of $CuCl_2{\cdot}2H_2O$ and 1.2mmol of TPP were dissolved into 5 mL of oleylamine in three-neck round bottom flask equipped with a condenser and attached to a Schlenk line. The reaction system was purged of argon at least by three cycles of evacuation. Under the argon atmosphere, the flask was immersed in an oil bath at 80°C for 20 min until the reaction mixture turned into the transparent blue liquid. Then, the flask was transferred to the oil bath at 170°C immediately. The blue liquid turned yellow after a few minutes and became black finally. The reaction system kept this temperature for 4 hours before it cooled to room temperature naturally in the air. The black powder was washed and separated by dispersing the reaction mixture in 2 mL chloroform and 10 mL ethanol, followed by centrifugation at 7000 rpm for 5 min.

The preparation process for spherical PdCu nanoparticles is similar to that of cubic PdCu particles. The amount of the TPP and oleylamine increased to 1.5mmol and 8ml. The black powder was washed firstly by centrifugation at 500rpm for 3min to remove some larger particles. Then, the liquid supernatant was washed by the same method of the PdCu cubes.

The final products were dispersed in chloroform for further characterization.

Synthesis of the Pd cubes

According to the previous reported method, 105 mg of PVP, 60 mg of AA, 300mg of KBr, and 8.0 mL of DI water were mixed in a 20 mL glass vial. The mixture was preheated to 80 °C for 10 min to dissolve all chemicals. Then 3 mL of prepared Na_2PdCl_4 in OLA (75mg for Na_2PdCl_4) was quickly injected into the preheated solution before the reaction kept 80°C for 3h.After the solution cooled to room temperature, the precipitate was washed with ethanol and acetone by centrifugation at 10000 rpm for 3 times, and then re-dispersed in ethanol for further use.

Acknowledgements

The work is sponsored by National Key R&D Program of China (No. 2017YFB0406000 and 2017YFA0303403), the National Science Foundation of China (21875137, 61974042, 51521004, and 51420105009), Innovation Program of Shanghai Municipal Education Commission (Project No. 2019-01-07-00-02-E00069), the 111 Project (Project No. B16032), and fund from Center of Hydrogen Science and Joint Research Center for Clean Energy Materials at Shanghai Jiao Tong University for financial supports. H.Z. acknowledges the financial support from Shanghai Automotive Industry Corporation (1714) and the computing resources from Shanghai Jiao Tong University Supercomputer Center. We also thanks ECNU Multifunctional Platform for Innovation (004) for characterization support.

Authors contribution

The manuscript was written through contributions of all authors. Q.Z. and J.W. conceived the idea and analyzed the experimental results. Q.Z. carried out the synthesis and the electrochemical test. F.L., L.L., and R.H. helped the characterization. F.L. and H.Z. simulated the results using the density functional theory (DFT) calculations. J.P. and W.Z. helped the synthesis process. W.C., Q.X., and F.S. helped to complete the electrochemical test. All authors have given approval to the final version of the manuscript.

Conflicts of interest

There are no conflicts to declare.

Keywords: intermetallic phases• electrocatalysts • fuel cells • oxygen reduction reaction • peroxide reduction

[1] J. Wu, H. Yang, *Acc. Chem. Res.* **2013**, *46*, 1848–1857.
[2] Z. Peng, H. Yang, *Nano Today* **2009**, *4*, 143–164.
[3] M. Shao, Q. Chang, J. P. Dodelet, R. Chenitz, *Chem. Rev.* **2016**, *116*, 3594–3657.
[4] J. Wu, J. Zhang, Z. Peng, S. Yang, F. T. Wagner, H. Yang, *J. Am. Chem. Soc.* **2010**, *132*, 4984–4985.
[5] J. Wu, L. Qi, H. You, A. Gross, J. Li, H. Yang, *J. Am. Chem. Soc.* **2012**, *134*, 11880–11883.
[6] X. Tian, X. Zhao, Y. Su, L. Wang, H. Wang, D. Dang, B. Chi, H. Liu, E. J. M. Hensen, X. W. Lou, B. Y. Xia, *Science* **2019**, *856*, 850–856.
[7] A. Chalgin, F. Shi, F. Li, Q. Xiang, W. Chen, C. Song, P. Tao, W. Shang, T. Deng, J. Wu, *CrystEngComm* **2017**, *19*, 6964–6971.
[8] Y. Ma, W. Gao, H. Shan, W. Chen, W. Shang, P. Tao, C. Song, C. Addiego, T. Deng, X. Pan, et al., *Adv. Mater.* **2017**, *29*, 1–8.
[9] J. Wu, A. Gross, H. Yang, *Nano Lett.* **2011**, *11*, 798–802.
[10] J. Wu, H. Yang, *Nano Res.* **2011**, *4*, 72–82.
[11] F. Li, Y. Qin, A. Chalgin, X. Gu, W. Chen, Y. Ma, Q. Xiang, Y. Wu, F. Shi, Y. Zong, et al., *ChemistrySelect* **2019**, *4*, 5264–5268.
[12] M. Luo, Z. Zhao, Y. Zhang, Y. Sun, Y. Xing, F. Lv, Y. Yang, X. Zhang, S. Hwang, Y. Qin, et al., *Nature* **2019**, *574*, 81–85.
[13] D. Wang, H. L. Xin, Y. Yu, H. Wang, E. Rus, D. A. Muller, H. D. Abruña, *J. Am. Chem. Soc.* **2010**, *132*, 17664–17666.
[14] F. Liao, T. W. B. Lo, S. C. E. Tsang, *ChemCatChem* **2015**, *7*, 1998–2014.
[15] M. Shao, T. Yu, J. H. Odell, M. Jin, Y. Xia, *Chem. Commun.* **2011**, *47*, 6566.
[16] T. C. Nagaiah, D. Schäfer, W. Schuhmann, N. Dimcheva, *Anal. Chem.* **2013**, *85*, 7897–7903.
[17] G. J. DeYulia, J. M. Cárcamo, O. Bórquez-Ojeda, C. C. Shelton, D. W. Golde, *Proc. Natl. Acad. Sci. U. S. A.* **2005**, *102*, 5044–5049.
[18] Y. Zhang, M. Janyasupab, C.-W. Liu, P.-Y. Lin, K.-W. Wang, J. Xu, C.-C. Liu, *Int. J. Electrochem.* **2012**, *2012*, 1–8.
[19] B. D. Adams, C. K. Ostrom, A. Chen, *J. Electrochem. Soc.* **2011**, *158*, 434–439.
[20] X. Sun, S. Guo, Y. Liu, S. Sun, *Nano Lett.* **2012**, *12*, 4859–4863.
[21] B. Li, J. Prakash, *Electrochem. Commun.* **2009**, *11*, 1162–1165.
[22] L. Arroyo-Ramírez, R. Montano-Serrano, T. Luna-Pineda, F. R. Román, R. G. Raptis, C. R. Cabrera, *ACS Appl. Mater. Interfaces* **2013**, *5*, 11603–11612.
[23] M. Neergat, V. Gunasekar, R. Rahul, *J. Electroanal. Chem.* **2011**, *658*, 25–32.
[24] M. H. Shao, K. Sasaki, R. R. Adzic, *J. Am. Chem. Soc.* **2006**, *128*, 3526–3527.
[25] Y. Dai, P. Yu, Q. Huang, K. Sun, *Fuel Cells* **2016**, *16*, 165–169.
[26] J. Wu, S. Shan, J. Luo, P. Joseph, V. Petkov, C. J. Zhong, *ACS Appl. Mater. Interfaces* **2015**, *7*, 25906–25913.
[27] J. Mao, Y. Liu, Z. Chen, D. Wang, Y. Li, *Chem. Commun.* **2014**, *50*, 4588–4591.
[28] W. P. Wu, A. P. Periasamy, G. L. Lin, Z. Y. Shih, H. T. Chang, *J. Mater. Chem. A* **2015**, *3*, 9675–9681.
[29] Y. Yang, C. Dai, D. Wu, Z. Liu, D. Cheng, *ChemElectroChem* **2018**, *5*, 2571–2576.
[30] Z. Yin, W. Zhou, Y. Gao, D. Ma, C. J. Kiely, X. Bao, *Chem. - A Eur. J.* **2012**, *18*, 4887–4893.
[31] L. Zhang, S. Il Choi, J. Tao, H. C. Peng, S. Xie, Y. Zhu, Z. Xie, Y. Xia, *Adv. Funct. Mater.* **2014**, *24*, 7520–7529.
[32] X. Wu, Q. Xu, Y. Yan, J. Huang, X. Li, Y. Jiang, H. Zhang, D. Yang, *RSC Adv.* **2018**, *8*, 34853–34859.
[33] A. Dasgupta, R. M. Rioux, *Catal. Today* **2019**, *330*, 2–15.
[34] Y. Yan, J. S. Du, K. D. Gilroy, D. Yang, Y. Xia, H. Zhang, *Adv. Mater.* **2017**, *29*, 1605997.
[35] C. Wang, D. P. Chen, X. Sang, R. R. Unocic, S. E. Skrabalak, *ACS Nano* **2016**, *10*, 6345–6353.
[36] K. Jiang, P. Wang, S. Guo, X. Zhang, X. Shen, G. Lu, D. Su, X. Huang, *Angew. Chem. Int. Ed.* **2016**, *55*, 9030–9035.
[37] Y. Qiu, L. Xin, Y. Li, I. T. McCrum, F. Guo, T. Ma, Y. Ren, Q. Liu, L. Zhou, S. Gu, et al., *J. Am. Chem. Soc.* **2018**, 1–20.
[38] C. Wang, X. Sang, J. T. L. Gamler, D. P. Chen, R. R. Unocic, S. E. Skrabalak, *Nano Lett.* **2017**, *17*, 5526–5532.
[39] L. Zhang, F. Hou, Y. Tan, *Chem. Commun.* **2012**, *48*, 7152–7154.
[40] J. T. L. Gamler, A. Leonardi, H. M. Ashberry, N. N. Daanen, Y. Losovyj, R. R. Unocic, M. Engel, S. E. Skrabalak, *ACS Nano* **2019**, *13*, 4008–4017.
[41] D. Wu, C. Dai, S. Li, D. Cheng, *Chem. Lett.* **2015**, *44*, 1101–1103.
[42] Q. Gao, Y. Ju, D. An, M. Gao, C. Cui, J. Liu, H.-P. Cong, S.-H. Yu, *ChemSusChem* **2013**, *6*, 1878–1882.
[43] M. Jin, H. Liu, H. Zhang, Z. Xie, J. Liu, Y. Xia, *Nano Res.* **2011**, *4*, 83–91.
[44] M. Shao, J. H. Odell, S. Il Choi, Y. Xia, *Electrochem. Commun.* **2013**, *31*, 46–48.
[45] S. Rudi, C. Cui, L. Gan, P. Strasser, *Electrocatalysis* **2014**, *5*, 408–418.
[46] J. Greeley, I. E. L. Stephens, A. S. Bondarenko, T. P. Johansson, H. A. Hansen, T. F. Jaramillo, J. Rossmeisl, I. Chorkendorff, J. K. Nørskov, *Nat. Chem.* **2009**, *1*, 552–556.
[47] X. Li, L. An, X. Wang, F. Li, R. Zou, D. Xia, *J. Mater. Chem.* **2012**, *22*, 6047–6052.
[48] Y. Xiong, H. Shan, Z. Zhou, Y. Yan, W. Chen, Y. Yang, Y. Liu, H. Tian, J. Wu, H. Zhang, et al., *Small* **2017**, *13*, 1603423.
[49] J. Wu, P. Li, Y. T. Pan, S. Warren, X. Yin, H. Yang, *Chem. Soc. Rev.* **2012**, *41*, 8066–8074.
[50] F. Xiao, Y. Li, X. Zan, K. Liao, R. Xu, H. Duan, *Adv. Funct. Mater.* **2012**, *22*, 2487–2494.
[51] M. Luo, Y. Sun, Y. Qin, S. Chen, Y. Li, C. Li, Y. Yang, D. Wu, N. Xu, Y. Xing, et al., *Chem. Mater.* **2018**, *30*, 6660–6667.
[52] H. S. Wroblowa, Yen-Chi-Pan, G. Razumney, *J. Electroanal. Chem. Interfacial Electrochem.* **1976**, *69*, 195–201.

[53] N. M. Marković, T. J. Schmidt, V. Stamenković, P. N. Ross, *Fuel Cells* **2001**, *1*, 105–116.
[54] J. K. Nørskov, J. Rossmeisl, A. Logadottir, L. Lindqvist, J. R. Kitchin, T. Bligaard, H. Jónsson, *J. Phys. Chem. B* **2004**, *108*, 17886–17892.
[55] Y. Sha, T. H. Yu, B. V. Merinov, W. A. Goddard, *ACS Catal.* **2014**, *4*, 1189–1197.
[56] W. Zhang, G. Fan, H. Yi, G. Jia, Z. Li, C. Yuan, Y. Bai, D. Fu, *Small* **2018**, *14*, 1703713.

.

Entry for the Table of Contents

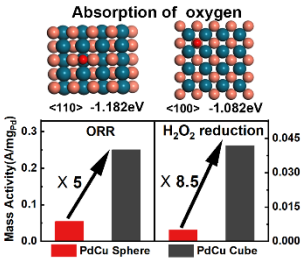

We synthesized PdCu intermetallic cubes and spheres to investigate the facet dependence on ORR and H_2O_2 reduction. The PdCu intermetallic cubes show up to 5 times and 8.5 times improvements in mass activity towards ORR and H_2O_2 reduction, compared with the PdCu intermetallic spheres. DFT calculation has uncovered that the dominant {100} faces of cubes had more appropriate oxygen adsorption and more thermodynamically favourable for H_2O_2 reduction than surface of spheres.